Quantitative MRI in obesity & reno-cardiovascular function

Dekkers, I.A.

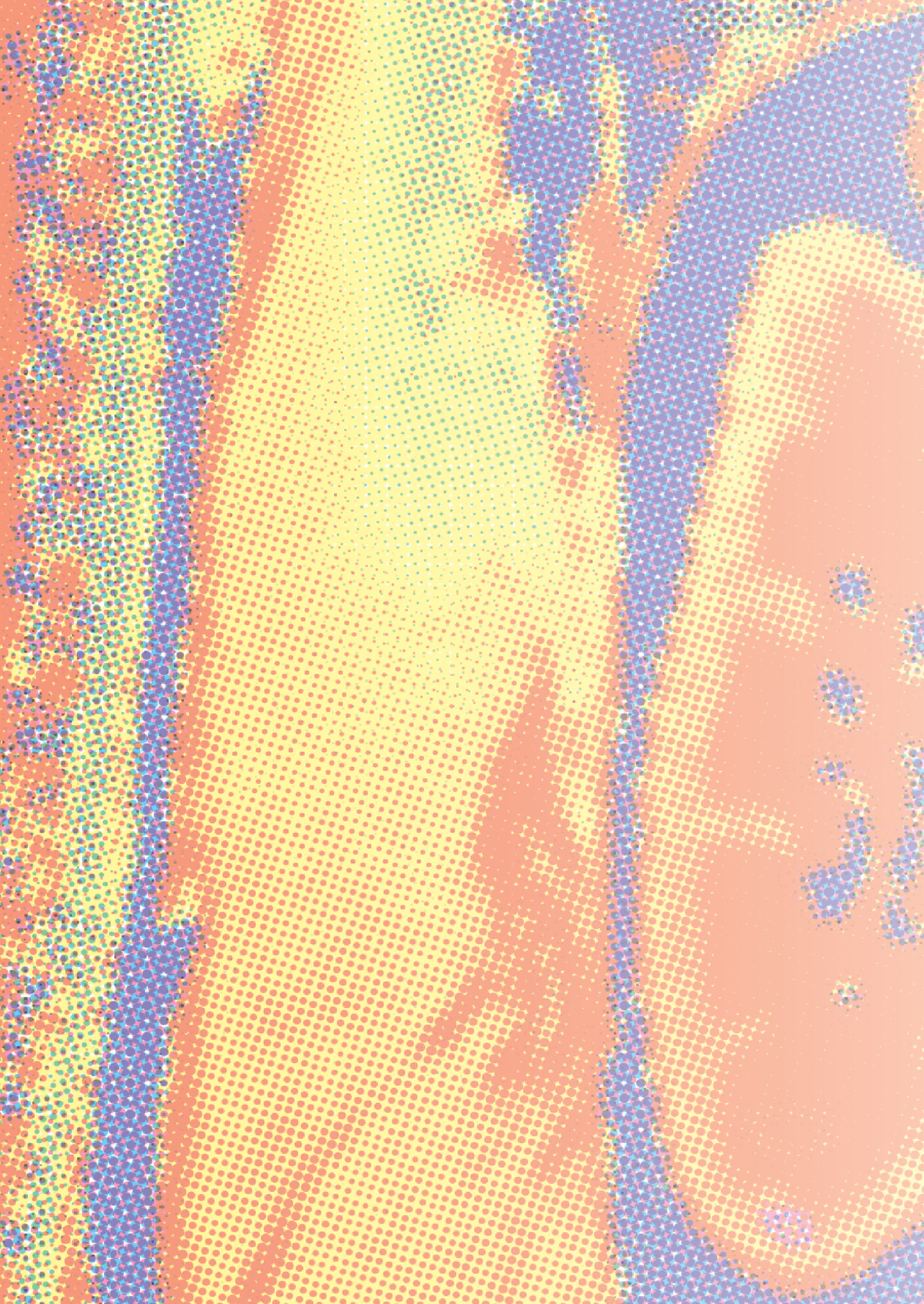

PART 1

Reproducibility and clinical validation studies

3

Reproducibility of Native T1-mapping for Renal Tissue Characterization using MOLLI at 3 Tesla

Dekkers IA, Paiman EHM, de Vries APJ, Lamb HJ.

J Magn Reson Imaging. 2019 Feb;49(2):588-96.

ABSTRACT

Background

Advanced renal disease is characterized by adverse changes in renal structure, however non-invasive techniques to diagnose and monitor these changes are currently lacking.

Objectives

Our aim was to assess the reproducibility of native T1 mapping for renal tissue characterization.

Methods

Fifteen healthy volunteers (mean age 31 ± 15 years, range 19–63 years), and 11 patients with diabetic nephropathy (mean age 57 ± 8 years, range 51–69 years) underwent renal T1 mapping using the Modified Look-Locker Imaging (MOLLI) 5(3)3 sequence at a 3T clinical MRI scanner. Intra- and inter-examination reproducibility of voxel based T1 relaxation times of renal cortex and medulla was assessed in healthy human volunteers and diabetic nephropathy patients. Reproducibility was evaluated using Bland-Altman and intra-class correlation coefficients (ICCs).

Results

Intra- and interexamination reproducibility of renal native T1 mapping showed good–strong ICCs (0.83–0.89) for renal cortex and medulla, and moderate–good ICCs (0.62–0.81) for cortex–medulla ratio in both healthy volunteers and diabetic nephropathy patients. Intra- and interexamination limits of agreement were respectively (–124 ms, +82 ms) and (–134 ms, +98 ms) for renal cortex and (–138 ms, +107 ms) and (–118 ms, +151 ms) for medulla. Overall T1 values for renal cortex ($P = 0.277$) and medulla ($P = 0.973$) were not significantly different between healthy volunteers and diabetic nephropathy patients, in contrast to the cortex–medulla ratio ($P = 0.003$).

Conclusion

Renal native T1 mapping is a technique with good–strong intra- and examination reproducibility in both healthy volunteers and diabetic nephropathy patients.

INTRODUCTION

Renal disease often progresses unnoticed as clinical parameters, such as glomerular filtration rate (GFR), tend to deteriorate only late in the disease course (1). There is an increasing need for the development of non-invasive imaging biomarkers that can help to predict clinical and functional outcomes in renal disease, and guide clinical decision making (2). Renal disease is characterized by adverse changes in both renal macrostructure (renal volume, and corticomedullary differentiation) and microstructure (renal inflammation, fibrosis, and lipid fat fraction) (3). These alterations in renal structure or renal tissue composition may be useful for differentiating specific renal disease states, and monitoring disease activity over time. Magnetic resonance imaging has the ability to discriminate tissue composition using T1 (spin-lattice) relaxation properties. Recent technical advances have enabled non-invasive tissue characterization via pixel-wise mapping of true T1 values of the target organ of interest, without the use of contrast agents. This so-called native T1 mapping, in which color-encoded pixel values represent the corresponding T1 relaxation times per voxel, has been used in cardiac MRI to visualize myocardial fibrosis, steatosis, edema, and hemosiderosis (4).

Previous clinical studies have shown that native T1 mapping could be helpful for identifying acute kidney injury and prediction of chronic kidney disease in mice (5–7). Additionally, recent clinical studies have showed promising results of renal native T1 mapping for the detection of fibrosis and prediction of graft functioning after kidney transplantation (8,9). Given the considerable influence of the imaging protocol, scanner, and patient related factors on measured T1 values, evaluation of reproducibility and robustness is critical (10).

The purpose of the present study was to evaluate the reproducibility of native T1 mapping for renal tissue characterization at 3T in healthy volunteers and diabetic nephropathy patients.

MATERIALS AND METHODS

Participants

The Institutional Review Board of our institution approved the study protocol for MR technique development, and written informed consent was obtained from all participants. Fifteen healthy volunteers (mean age 31 ± 15 years, range 19–63, 67% male) without known renal disease agreed to participate in the current study and were recruited from a database of healthy volunteers who regularly participate in technical MRI development studies. Eleven subjects with a known history of diabetic nephropathy (mean age 57 ± 8 years, range 51–69, 80% male, urinary albumin excretion ratio >2.5 mg/mmol for men or

>3.5 mg/mmol for women, and estimated GFR >60ml/min/1.73m²) agreed to participate in the present study and were recruited from a database of past clinical trial participants.

Data acquisition

MR examinations were performed at a 3T clinical MRI scanner (Ingenia, Philips, Best, The Netherlands). The standard cardiac/body coil was used for transmission with two arrays (anterior and posterior with respectively 16 and 12 elements) for reception. After a breath-hold survey was obtained, three orthogonal modified Dixon scans were acquired of the left kidney. T1 mapping was performed using the modified Look-Locker inversion-recovery (MOLLI) sequence at the center of the kidney in sagittal orientation (**Fig. 1a**). The sagittal orientation was chosen as this orientation is less prone to through-plane volume effects compared to the coronal orientation while maintaining an overview of the upper and lower poles of the kidney which is useful for assessing potential local differences. Breath-holds were used for respiratory motion compensation. A turbo field echo (TFE) prepulse with an inversion delay of 350 ms was the longest (and last) inversion delay in the MOLLI scheme. Other inversion times in the MOLLI scheme were equidistantly distributed between shortest and longest value, according to the 5(3)3 cardiac MR protocol. Since the cardiac 5(3)3 protocol is normally electrocardio-graphically gated, we used the physiology simulator (Philips) to ensure scan triggering by simulating cardiac triggering in order to apply the protocol for renal imaging. The shortest inversion time was used for the first part of the MOLLI scheme, and depended on the TFE shot duration which is around 100 ms. Finally, 8 images were acquired, and in-line motion correction and map generation were performed. Used readout parameters were: slice thickness 8 mm, spacing between slices 8 mm, field of view 300 x 300 mm; matrix 256 x 256 x 1 slice; pixel size 1.17 x 1.17 mm. Intra-examination reproducibility measurements were obtained by repeating the scan without repositioning of the subject or changing the position of the surface coil or measurement volumes. Inter-examination reproducibility was assessed on the same day after removal and repositioning of subject in the magnet, and repositioning of the surface coil and measurements volumes. Inter-examination scans were added later in the scan protocol and were therefore not assessed in all healthy volunteers. Total acquisition time including positioning of the subject, scanning preparatory sequences, planning and data acquisition was on average 4 minutes.

T1 mapping quantification

Eight T1-weighted source images were taken at different times (ms) after an inversion pulse at time t=0 for MOLLI 5(3)3 during a single breath-hold (**Fig. 1b**). Post-processing was done using QMap Research Edition (Medis, Leiden, the Netherlands) using received data in DICOM format. Inversion recovery curves were constructed for renal cortex (orange) and medulla (red) based on MOLLI images with varying effective inversion time

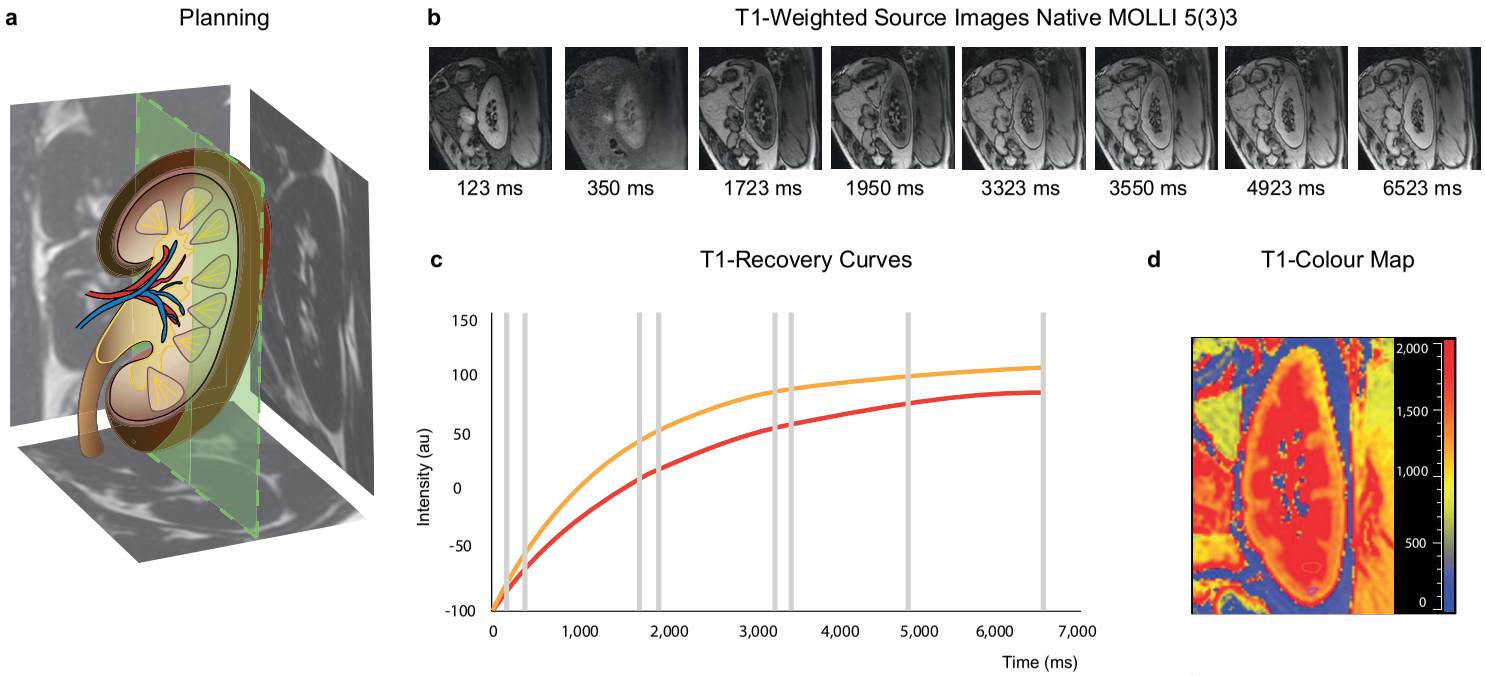

Figure 1. Planning and acquisition protocol of native MOLLI 5(3)3. (**a**) Planning of T1-mapping in the sagittal plane based on three orthogonal on mDixon images. (**b**) T1-weighted source images in sagittal plane taken at different times (ms) after an inversion pulse at time t=0 for MOLLI 5(3)3 all acquired during a single breath-hold. (**c**) Inversion recovery curves for renal cortex (orange) and medulla (red) generated from the source images. (**d**) Generated color-encoded T1 map in which pixel values represent corresponding T1 relaxation times per voxel.

(TI) with one series containing multiple images (**Fig. 1c**). The T1 mapping curve fitting to a three-parameter nonlinear cuve can be described as (y=A-B*exp(-TI/T1*) and correction (T1=T1*(B/A-1)) (11).

Offset, scaling, and T1 were calculated via fitting the algorithm at each pixel {x,y}, resulting in additional offset, scaling and T1 maps. The color-encoded pixel based T1 maps provide a quantitative visualization of the tissue T1 properties since the signal intensity of each pixel directly reflects the relaxation time calculated in milliseconds (**Fig. 1d**). The offset, scaling and T1 maps were used to calculate additional R2 and residual maps for quality control, where good quality is reflected by R2 values and low residual values. The R2 and residual error map are sensitive for poor fitting due to motion related artifacts, and spatial variation in off resonance due to B0-field inhomogeneity (**Fig. 2**) In case necessary manual motion correction was performed.

Freehand region of interest (ROI) based measurements were made for the mean T1 values by manually drawing small sample ROIs in the renal cortex and medulla of the lower pole of the left kidney (**Fig. 2**). Both renal cortex and medulla showed minimal regional differences and limited variance (SD) of the small sample ROI measurements. Outer borders of the kidney were not included in ROI measurements, since the outer border between renal parenchyma and perirenal fat or renal sinus fat are prone to gradual changes in T1 values due to partial volume averaging artifacts and possible residual registration error after motion correction. Regions with banding artifacts in the kidney due to off-resonance were also avoided for ROI measurement, since these artifacts can cause significant error at relatively small off-resonance frequencies (12). The cortex-medulla ratio was determined by dividing the (ROI-based) native T1 value of renal cortex by the native T1 value of the medulla.

Statistical analysis

T1 values and other descriptors are presented as mean (SD), range, and percentage. The Shapiro-Wilk test and assessment of histogram plots was applied to determine whether the data was normally distributed and to select appropriate parametric tests. Pearson's correlation, and intra-class correlation coefficients (ICC) were calculated for intra- and inter-examination measurements. The ICC can be interpreted as the ratio of the between subject variance compared to the total variance (sum of the between subject and within subject variances), and was computed using a two-way mixed effects model (13). Agreement was classified as follows: ICC >0.95; excellent, 0.95–0.85; strong, 0.85–0.70; good, 0.70–0.50; moderate, <0.5; poor. Bland-Altman plots were constructed for intra- and inter-examination measurements and were visualized through a scatterplot of the differences, with reference lines at the mean difference, and mean difference ± 2 × standard deviation of the differences (limits of agreement) (14).

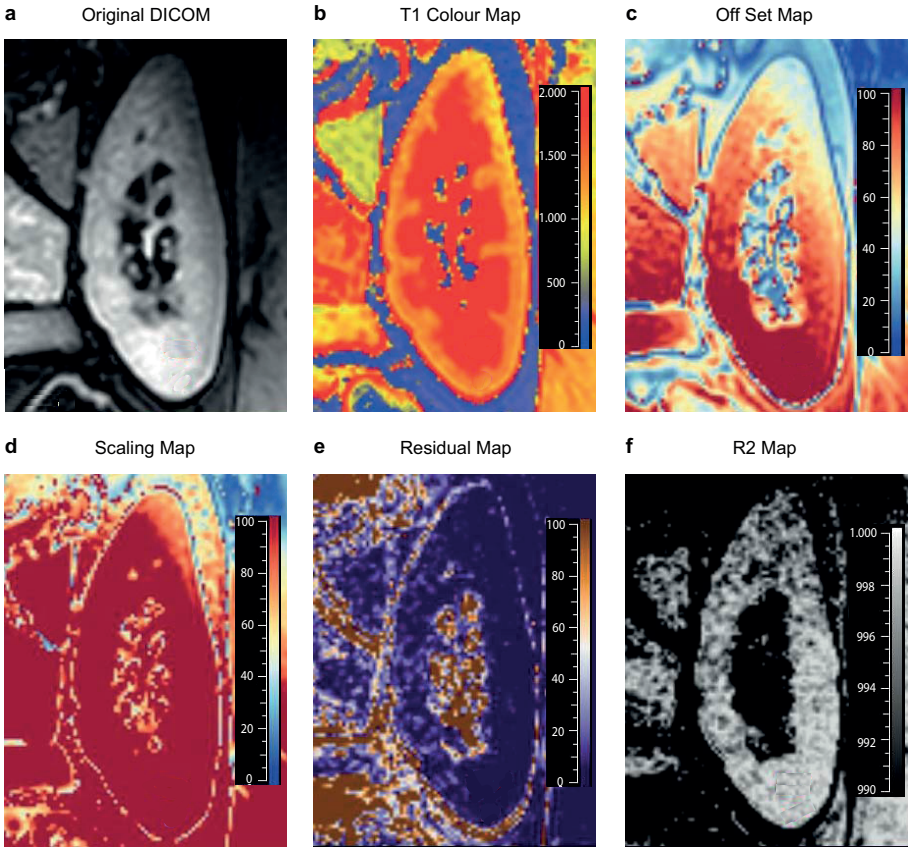

Figure 2. Region of interest measurements for renal cortex and medulla on original DICOM, T1 Colour Map, Offset Map, Scaling Map, Residual Map, R2 Map.(**a**) Original DICOM image of the MOLLI 5(3)3 sequence in sagittal plane of the left kidney, (**b**) Color-encoded pixel based T1 map (**c**) Offset map corresponds to the plateau value of the function which should be equal to the last time point of the MOLLI 5(3)3 sequence, (**d**) Scaling map which ideally should have be twice the value of the offset because than the T1 is equal to the apparent recovery time T1*, (**e**) residual map reflects the sum of squared differences between the fitted intensity value and the original image normalized for the number of image frames, (**d**) R2 map corresponds to the coefficients of determination, which lies between 0 and 1000 since the DICOM images store only integer values.

Two-tailed $P<0.05$ was considered to indicate a statistically significant difference. Statistical analyses were performed using STATA version 12.0 (Statacorp, College Station, Texas).

RESULTS

The overall results regarding the mean T1-values, Pearson correlation and ICCs for first, intra- and inter-examination scans are presented in **Table 1**. Overall mean T1 values

Table 1. Mean T1-values, Pearson correlation and ICCs for first, intra- and inter-examination scans.

	Healthy volunteers			Diabetic Nephropathy patients			Combined		
	Scan 1 n=15	Intra-examination scan n=15	Inter-examination scan n=9	Scan 1 n=11	Intra-examination scan n=11	Inter-examination scan n=11	Scan 1 n=26	Intra-examination scan n=26	Inter-examination scan n=20
T1 value (ms)									
Cortex	1408 ± 80	1437 ± 78	1427 ± 62	1433 ± 88	1445 ± 82	1449 ± 80	1419 ± 83	1440 ± 78	1861 ± 85
Medulla	1882 ± 108	1912 ± 83	1923 ± 63	1850 ± 89	1846 ± 100	1810 ± 65	1868 ± 100	1883 ± 95	1439 ± 72
CM ratio	0.75 ± 0.05	0.75 ± 0.03	0.74 ± 0.04	0.77 ± 0.03	0.78 ± 0.03	0.80 ± 0.04	0.76 ± 0.04	0.77 ± 0.03	0.77 ± 0.05
Pearson correlation (r)									
Cortex		0.65	0.49		0.96	0.79		0.80	0.71
Medulla		0.80	0.88		0.85	0.66		0.80	0.71
CM ratio		0.36	0.65		0.38	0.58		0.45	0.70
ICC (95% CI)									
Cortex	0.79 (0.37, 0.93)		0.66 (-0.51, 0.86)	0.98 (0.93, 0.99)		0.88 (0.55, 0.97)	0.89 (0.75, 0.95)		0.83 (0.56, 0.93)
Medulla	0.87 (0.62, 0.96)		0.91 (0.56, 0.98)	0.91 (0.70, 0.98)		0.77 (0.14, 0.94)	0.89 (0.76, 0.95)		0.83 (0.57, 0.93)
CM ratio	0.52 (-0.44, 0.84)		0.79 (0.06, 0.95)	0.55 (-0.57, 0.87)		0.70 (-0.14, 0.92)	0.62 (0.16, 0.83)		0.81 (0.52, 0.93)

T1 values are expressed as mean ± SD. CM ratio; cortex-medulla ratio. ICC; intra-class correlation coefficient.

of healthy volunteers were 1418 ± 73 ms (range 1270–1482 ms) for renal cortex and 1886 ± 86 ms (range 1695–2006 ms) for medulla. Overall mean T1 values of diabetic nephropathy patients were 1445 ± 81 ms (range 1392–1545 ms) for renal cortex and 1840 ± 79 ms (range 1751–2003 ms) for medulla. The overall mean cortex-medulla ratio was 0.75 ± 0.03 (range 0.70–0.80) for healthy volunteers and 0.79 ± 0.03 (range 0.74–0.82) for diabetic nephropathy patients. No significant differences were present when comparing T1 values for renal cortex (*P*=0.277) and medulla (*P*=0.73) of healthy volunteers with diabetic nephropathy patients. The cortex–medulla ratio was significantly different between healthy volunteers and diabetic nephropathy patients (*P*=0.003) (**Fig. 3**). Intra- and inter-examination measurements were highly correlated with first T1 value measurements of renal cortex and medulla.

Intra-examination ICCs of renal cortex and medulla for both healthy volunteers and diabetic nephropathy patients combined were respectively 0.89 (95% CI 0.75, 0.95) and 0.89 (95% CI 0.76, 0.95). Inter-examination ICCs for renal cortex and medulla were 0.83 (95% CI 0.56, 0.93) and 0.83 (95% CI 0.57, 0.93). The cortex-medulla ratio had an intra-examination ICC of 0.62 (95% CI 0.16, 0.83) and 0.81 (95% CI 0.52, 0.93).

The Bland-Altman lower and upper limits of agreement for intra-examination and inter-examination T1 measurements of renal cortex were respectively -124 ms (95% CI -159, -88) and 82 ms (95% CI 47, 118), and -134 (95% CI -181, -87) and 98 ms (95% CI -51, 145) (**Fig. 4a and Fig. 4b**). Intra- and inter examination Bland-Altman lower and upper limits of agreement for renal medulla were -138 ms (95% CI -180, -96), 107 ms (95% CI 65, 149) (**Fig. 4c and Fig. 4d**), and -118 ms (95% CI -172, -63), 151 ms (95% CI 96, 205). Cortex-medulla ratio measurements had lower and upper limits of agreement of -0.08 (95% CI -0.11, -0.06) and 0.07 (95% CI 0.05, 0.10) for intra-examination measurements, and -0.09 (95% CI -0.12, -0.06) and 0.06 (95% CI 0.03, 0.08) for inter-examination measurements (**Fig. 4e and Fig. 4f**).

To illustrate the potential application of renal T1 mapping, we have visualized coronal renal T1 maps of a healthy volunteer (left), and renal transplant recipient (right) in **Figure 5**. The renal T1 map the healthy volunteer has T1 values of 1468 ms in the renal cortex, and 1941 ms for medulla (cortex–medulla ratio of 0.76), compared to native T1 values of 1658 ms for renal cortex and 1951 ms for medulla (cortex–medulla ratio of 0.85) in the transplanted kidney.

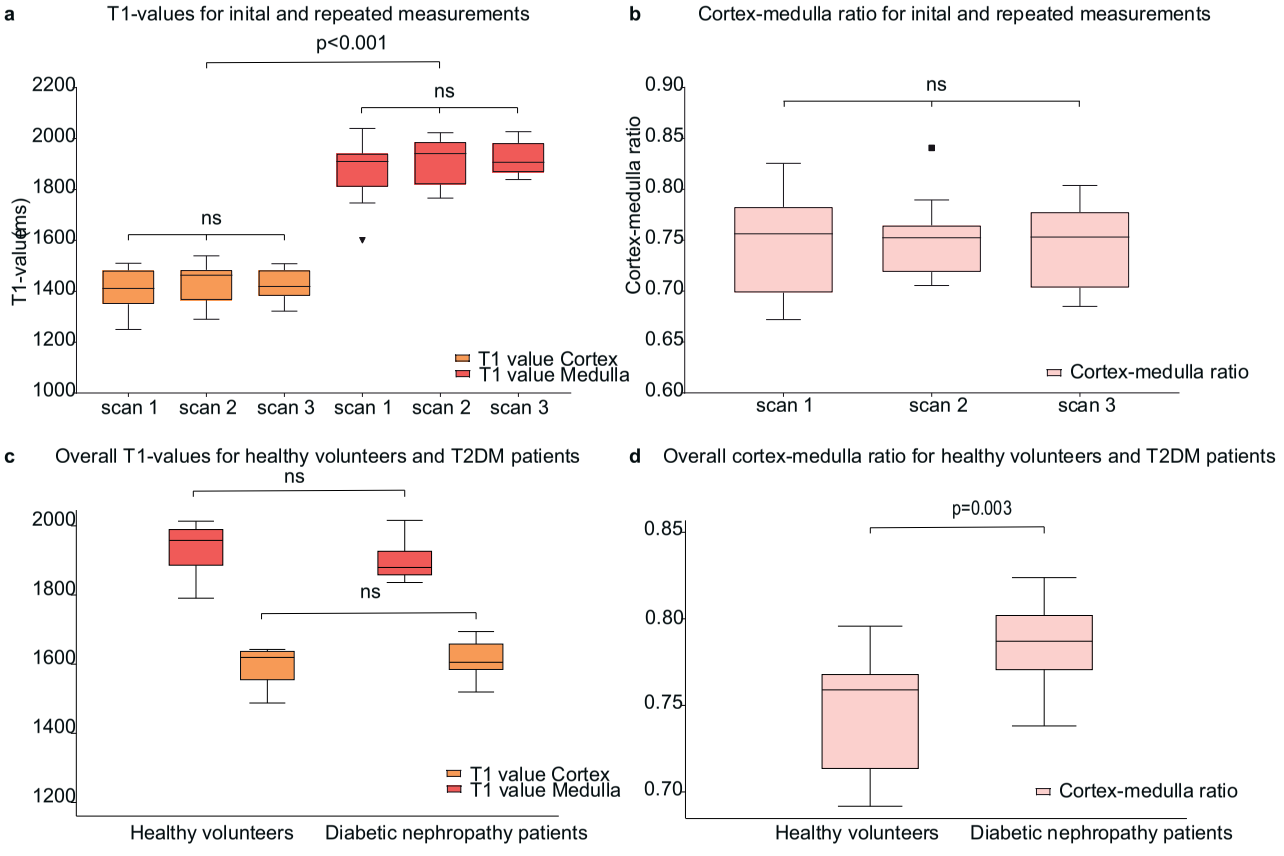

Figure 3. Distribution of MOLLI 5(3)3 ROI based T1 values of renal cortex, medulla and cortex-medulla ratio for first, intra- and inter-examination measurements. (**a**) Distribution of T1 values of renal cortex (orange) and medulla (red) for first scan and repeated intra- and inter-examination scans in healthy volunteers. (**b**) Distribution of cortex-medulla ratio based on first scan and repeated intra- and inter-examination scans in healthy volunteers.

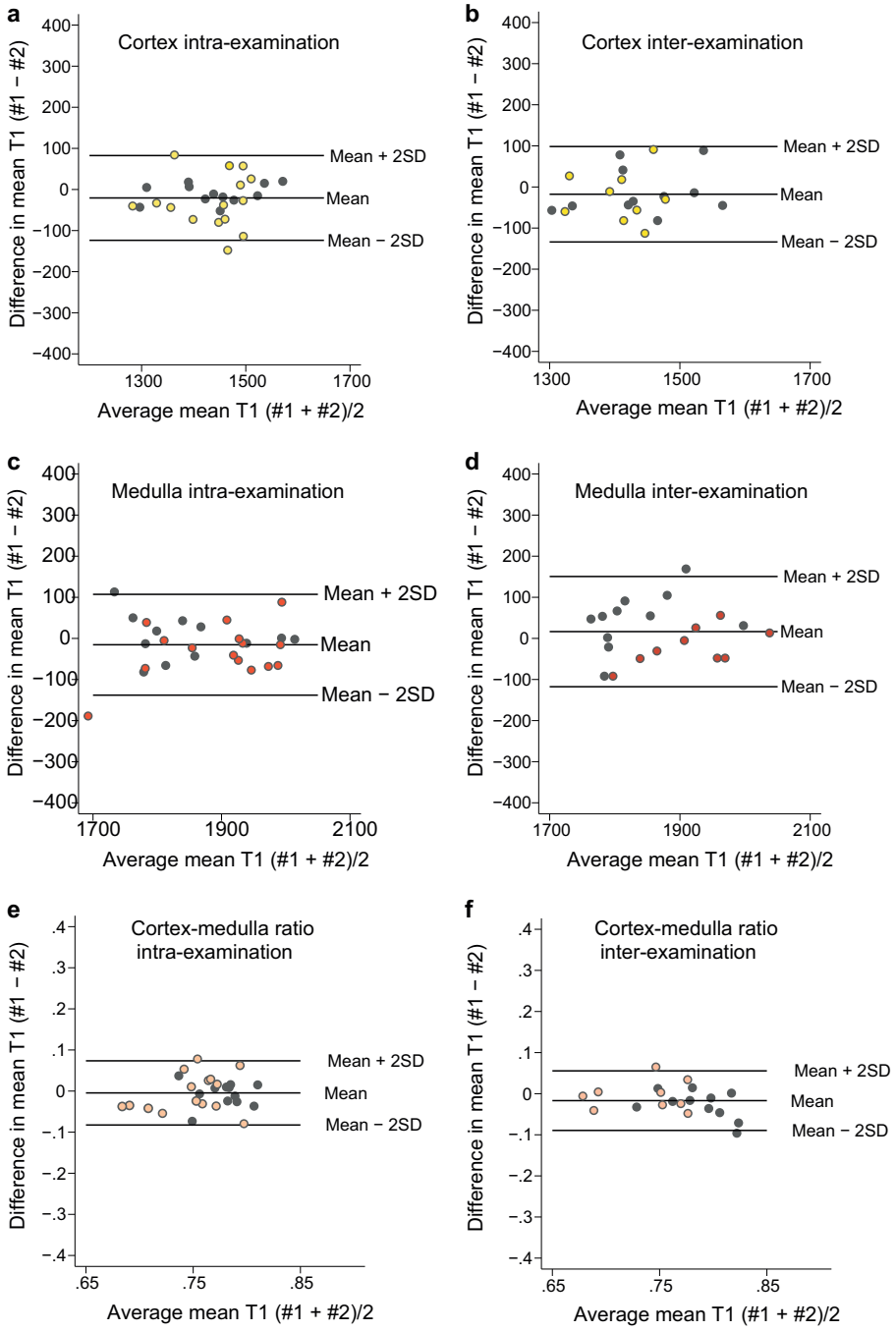

Figure. 4. Bland-Altman Plots of intra-examination and inter-examination T1-measurements of renal cortex, medulla and cortex-medulla ratio in healthy volunteers (in color) and diabetic nephropathy patients (in black).

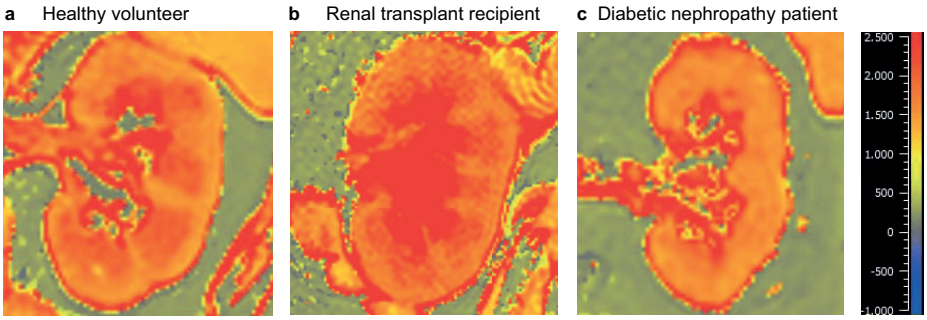

Figure 5. Coronal T1 map of a healthy volunteer (left), a renal transplant recipient (middle), and a patient with diabetic nephropathy (right). (**a**) T1 map of a kidney of a healthy volunteer in coronal view with values of 1468 ms for renal cortex, 1941ms for medulla, and a cortex-medulla ratio of 0.76. (**b**) T1 map of a renal transplant patient with an eGFR of 56 ml/min/1.73m² at time of scanning, native T1 values were of 1658 ms for renal cortex, 1951 ms for medulla, and a cortex-medulla ratio of 0.85. (**c**) T1 map of a patient with diabetic nephropathy showing a diminished cortico-medullary differentiation.

DISCUSSION

We demonstrated that renal native T1 mapping using the MOLLI 5(3)3 sequence is a reproducible technique that could be used for renal tissue characterization.

The intra- and inter-examination reproducibility of measured renal T1 values are an important determinant of the clinical utility of pixel-wise T1 mapping for disease assessment. We evaluated the reproducibility of T1 measurements in renal cortex, renal medulla and for the cortex-medulla ratio. Both intra- and inter-examination ICCs ranged between moderate–strong in healthy volunteers and diabetic nephropathy patients separately. Intra- and inter examination ICCs for both groups combined were respectively 0.89 and 0.83 for both renal cortex and renal medulla indicating strong intra-examination reproducibility. This is supported by the Bland-Altman plots showing good agreement. One outlier was present in the intra- and inter-examination Bland-Altman plots, which is likely the same healthy volunteer with residual motion artefacts due to non-compliance to breath-hold instructions during the data acquisition of scan 1. In general, ICC values were higher for renal medulla compared to cortex. The cortex is likely more sensitive for trough-plane partial volume effects than the medulla based on its anatomical borders and relatively limited thickness. This could potentially be improved via high resolution 3D T1 mapping or via the use of post-processing techniques such as automated motion correction of residual motion artefacts. The cortex-medulla ratio had ICCs ranging between moderate–good, indicating that this is a less reliable measure than T1 values directly measured in renal cortex and medulla.

Conventional MR imaging of the kidney clearly demonstrates anatomical differences between renal cortex and medulla due to the shorter T1 relaxation times of the cortex.

Loss of this so-called corticomedullary differentiation occurs in several renal diseases and has been primarily attributed to altered T1 relaxation times in the renal cortex (15). Determination the cortex-medulla ratio using true native T1 values of renal cortex and medulla enables quantification of the corticomedullary differentiation, which might be useful for differentiating specific renal disease states, such as renal fibrosis. In the present study T1 values of the cortex ranged between 1270–1482 ms, compared to 1695–2006 ms for medulla in healthy volunteers at 3T. Since native T1 values are considered to reflect both cellular components as interstitium, we postulate that the found differences between cortical and medullary T1 values convey anatomical differences in the renal (tubular) interstitium, which is defined as the extravascular, extraglomerular and (inter)tubular space of the kidney (16). Renal interstitial volume, in contrast to severity of glomerular disease, is highly correlated with kidney function, (17,18) and can occupy over 60% of kidney tissue in severe renal disease (19,20). Recently, it has been showed by Friedli et al. that renal native T1 values correlate well with renal fibrosis stage based on histology, suggesting that native renal T1 might be a useful parameter to detect (subclinical) renal fibrosis (8). Another very recent study in renal transplant recipients found prolonged T1 values after transplantation and increased cortical T1 values in higher stages of renal functional impairment (9), indicating the potential use for prediction of graft survival/functioning. However, to what extent native T1 mapping could be used as a safe non-invasive alternative for diagnosis and follow-up of renal disease, remains to be further investigated.

Several limitations are present in this study that need to be considered. Since native T1 mapping is at least partially modulated by perfusion (which is also a major determinant of GFR), T1 relaxation times obtained in patients with impaired renal function could potentially be confounded by lower renal perfusion rather reflecting true fibrosis only. This could also have important implications when other T1-mapping based techniques are used such as arterial spin labelling, which could potentially limit the application of these techniques in the kidney. More research is needed to determine to what extent native renal T1 values are affected by altered perfusion, however we expect that current reproducibility measurements are minimally influenced by differences in renal perfusion since the study population consists of healthy volunteers and diabetic nephropathy patients with an eGFR >60ml/min/1.73m^2. In the present study the aim was to evaluate the reproducibility of renal T1 mapping rather than evaluating the differences between healthy volunteers and renal disease patients, as this would have required a much larger sample size encompassing a wide variety with renal disease patients as chronic kidney disease is a highly heterogeneous disease group with different underlying pathologies and stages (21). We hypothesize that certain specific renal diseases (e.g. focal and diffuse fibrosis, and renal infiltrative diseases such as renal involvement in Fabry disease) might potentially benefit form renal T1 mapping while others may not, based on the underlying

disease-specific changes in renal tissue composition. Native renal T1 mapping could be of added value to the renal diagnostic arsenal considering it facilitates direct quantification of renal tissue and enables assessment of regional variances. To what extent renal T1 mapping could truly influence clinical decision-making compared to currently available renal function markers and other new MR techniques such as diffusion weighted imaging, and blood-oxygen-level dependent imaging remains to be investigated, and further histological validation of renal T1 mapping for tissue characterization is warranted. In the present study we used the same 5(3)3 MOLLI scheme as in cardiac MR imaging because of practical advantages for clinical implementation. However other T1 mapping acquisition protocols might provide more accurate renal T1 measurements since MOLLI measurements are known to be influenced by T2-dependence, magnetization transfer effect, and inversion efficiency (22). Although automated parametric mapping using dedicated software minimizes user-dependent influences, we cannot completely exclude possible intra- and inter-observer variation in the current measurements. Further research is needed to correlate renal native T1-values with disease severity based on histopathology, and whether renal native T1 mapping has added value for clinical decision making. In addition, more studies are needed to assess the reproducibility of renal native T1 mapping at different imaging centers with various MRI scanner manufacturers, in order to compare current measurements to other centers and to establish normal reference values.

In conclusion, renal native T1-mapping is a promising technique for renal tissue characterization with good–strong intra- and inter-examination reproducibility. Further research is needed to correlate renal native T1-values with histologic disease severity, and to determine the impact on clinical decision making.

REFRENCES

1. Porrini E, Ruggenenti P, Mogensen CE, et al. ERA-EDTA diabesity working group. Non-proteinuric pathways in loss of renal function in patients with type 2 diabetes. Lancet Diabetes Endocrinol 2015;3: 382–391
2. O'neill WC. Structure, not just function. Kidney Int 2014;85:503–505.
3. Grenier N, Merville P, Combe C. Radiologic imaging of the renal parenchyma structure and function. Nat Rev Nephrol 2016;12:348–359.
4. Taylor AJ, Salerno M, Dharmakumar R, Jerosch-Herold M. T1 mapping: Basic techniques and clinical applications. JACC Cardiovasc Imaging 2016;9:67–81.
5. Hueper K, Peperhove M, Rong S, et al. T1-mapping for assessment of ischemia-induced acute kidney injury and prediction of chronic kidney disease in mice. Eur Radiol 2014;24:2252–2260.
6. Hueper K, Hensen B, Gutberlet M, et al. Kidney transplantation: Multiparametric functional magnetic resonance imaging for assessment of renal allograft pathophysiology in mice. Invest Radiol 2016;51:58–65.
7. Tewes S, Gueler F, Chen R, et al. Functional MRI for characterization of renal perfusion impairment and edema formation due to acute kidney injury in different mouse strains. PLoS One 2017;12:e0173248.
8. Friedli I, Crowe LA, Berchtold L, et al. New magnetic resonance imaging index for renal fibrosis assessment: A comparison between diffusion-weighted imaging and T1 mapping with histological validation. Sci Rep 2016;6:30088.
9. Peperhove M, Vo Chieu VD, Jang MS, et al. Assessment of acute kidney injury with T1 mapping MRI following solid organ transplantation. Eur Radiol 2018;28:44–50.
10. Kellman P, Hansen MS. T1-mapping in the heart: accuracy and precision. J Cardiovasc Magn Reson 2014;16:2.
11. Messroghli DR, Radjenovic A, Kozerke S, Higgins DM, Sivananthan MU, Ridgway JP. Modified Look-Locker inversion recovery (MOLLI) forhigh-resolution T1 mapping of the heart. Magn Reson Med 2004;52:141–146.
12. Kellman P, Herzka DA, Arai AE, Hansen MS. Influence of Offresonance in myocardial T1-mapping using SSFP based MOLLI method. J Cardiovasc Magn Reson 2013;15:63.
13. McGraw KO, Wong SP. Forming inferences about some intraclass correlation coefficients. Psychol Methods 1996;1:30.
14. Bland JM, Altman DG. Statistical methods for assessing agreement between two methods of clinical measurement. Lancet 1986;1:307–310.
15. Lee VS, Kaur M, Bokacheva L, et al. What causes diminished corticomedullary differentiation in renal insufficiency? J Magn Reson Imaging 2007;25:790–795.
16. Lemley KV, KRIz W. Anatomy of the renal interstitium. Kidney Int 1991;39:370–381.

17. Bohle A, Grund KE, Mackensen S, Tolon M. Correlations between renal interstitium and level of serum creatinine. Morphometric investigations of biopsies in perimembranous glomerulonephritis. Virch Arch A Pathol Anat Histol 1977;373:15–22.

18. Bohle A, von Gise H, Mackensen-Haen S, Stark-Jakob B. The obliteration of the postglomerular capillaries and its influence upon the function of both glomeruli and tubuli. Functional interpretation of morphologic findings. Klin Wochenschr 1981;59:1043–1051.

19. Zeisberg M, Kalluri R. Physiology of the renal interstitium. Clin J Am Soc Nephrol 2015;10:1831–1840.

20. Nath KA. Tubulointerstitial changes as a major determinant in the progression of renal damage. Am J Kidney Dis 1992;20:1–17.

21. Levey AS, Coresh J. Chronic kidney disease. Lancet 2012;379:165–180.

22. Roujol S, Weingartner S, Foppa M, et al. Accuracy, precision, andreproducibility of four T1 mapping sequences: A head-to-head comparison of MOLLI, ShMOLLI, SASHA, and SAPPHIRE. Radiology 2014;272:683–689.